

Strategy for Planning Accelerated Life Tests with Small Sample Sizes

Haiming Ma and W. Q. Meeker
Department of Statistics
Iowa State University
Ames, IA 50011

Abstract

Previous work on planning accelerated life tests has been based on large-sample approximations to evaluate test plan properties. In this paper, we use more accurate simulation methods to investigate the properties of accelerated life tests with small sample sizes where large-sample approximations might not be expected to be adequate. These properties include the simulated s-bias and variance for quantiles of the failure-time distribution at use conditions. We focus on using these methods to find practical compromise test plans that use three levels of stress. We also study the effects of not having any failures at test conditions and the effect of using incorrect planning values. We note that the large-sample approximate variance is far from adequate when the probability of zero failures at certain test conditions is not negligible. We suggest a strategy to develop useful test plans using a small number of test units while meeting constraints on the estimation precision and on the probability that there will be zero failures at one or more of the test stress levels.

Key Words – Large-Sample Approximate Variance, Maximum likelihood, Reliability, Simulation.

Acronyms

ALT	accelerated life test
ZFP1	problem when zero failures occur at one or more levels of stress
ZFP2	problem when zero failures occur at two or more levels of stress
ML	maximum likelihood
CPPV	critical point planning values

Notation

n	total number of test units
s_U, s_H	pre-specified use level and highest level of stress
s_L, s_M	lowest and middle levels of stress
π_L, π_M, π_H	allocations of test units at s_L, s_M and s_H , respectively
ξ	standardized stress level $\xi = (s - s_U)/(s_H - s_U)$
t, η	failure time and censoring time
μ, σ	location and scale parameters of a location-scale distribution
γ_0, γ_1	parameters of the log-linear regression model
$\phi(\cdot), \Phi(\cdot)$	standard pdf and cdf, respectively, of a location-scale distribution
p_U, p_L, p_M, p_H	probabilities that a unit will fail by time η at use, lowest, middle and highest stress levels, respectively
$\pi_L^E, (\xi_L^E)$	allocation (lowest level of stress), corresponding to having an equal expected number of failures at each of the three levels of stress for a fixed value of ξ_L (π_L).

$\pi_L^{Opt}, (\xi_L^{Opt})$	allocation and lowest level of stress, respectively, corresponding to overall optimum (minimum) variance of the quantile estimators obtained by adjusting π_L and ξ_L , simultaneously.
z_p	p quantile of a standard location-scale distribution
$y_p = y_p(\xi)$	p quantile of a location-scale distribution at stress level ξ

1 Introduction

1.1 Previous work

In an accelerated life test (ALT), units are tested at higher than usual levels of stress (e.g., temperature, voltage, or pressure) to obtain information about reliability in a small amount of time. ALTs are commonly used in product design and testing processes (see, for example, Chapter 6 of Nelson [11] and Chapters 18-20 of Meeker and Escobar [9]). Previous ALT planning methods have been based on large-sample approximations to assess test plan properties. The test plan properties (and corresponding approximations) depend on the model parameters. Thus one needs planning values for the parameters. As suggested in [5], the planning values can be given in terms of convenient quantities such as failure probabilities at the highest and use stress levels, respectively. As suggested in [12] and [13] information for planning values can be obtained from previous experience with similar products and materials or engineering judgment. Optimized two-stress-level test plans based upon such planning values that achieve the smallest large-sample approximate variance of the maximum likelihood (ML) estimators of interest (see, for example, ref. [9, 11 and 13]) have been studied extensively. To be robust to possible misspecification of the planning values and the relationship between the life and the levels of accelerating stress, compromise test plans with three or more levels have also been proposed and applied in practice [3, 7, 9 and 12].

1.2 Motivation

In practice, ALTs are usually subject to the constraint that the available number of test units has to be small either because of high cost of the units or availability of prototype units. In these cases, test planners may need to know the smallest possible number of units that are needed and how to choose the levels of stress and the allocation for those units to achieve a specified precision in the ML estimators.

We show how to find practical, statistically efficient constant-stress ALT plans with three levels of stress. When the sample sizes are small, test plans generated from large-sample approximations may not be adequate. In this paper, we use large-sample approximations for initial guidance but turn to simulation to do the needed evaluation of the properties of small-sample test plans that are needed to choose an actual plan. We illustrate the methods with an example. The results show that ALT test plans for small samples can be distinctly different from those suggested by large-sample approximations.

1.3 Overview

The remainder of this paper is organized as follows. Section 2 presents the model upon which our evaluations are based and introduces an ALT example that we use to illustrate how to evaluate the test-plan properties with small samples. Section 3 evaluates optimized compromise test plans with small samples. Section 4 studies test plans with the smallest zero failure probability and considers the impact of using incorrect planning values. Section 5 investigates the effect that using a small sample size will have on the adequacy of normal-approximation confidence intervals. Section 6 gives some concluding remarks and describes related areas for future research.

2 Model and MI Estimation

2.1 Setup

As described in [3] and [11], most ALT models require a transformation of stress (e.g., log of voltage). We use s to denote this transformed stress. All of the stress levels in the ALT will be between the use stress s_U and a pre-specified highest stress s_H . For convenience, we use the standardized stress $\xi = (s - s_U)/(s_H - s_U)$, where $s_U \leq s \leq s_H$ and $0 \leq \xi \leq 1$. Thus $\xi_U = 0$ and $\xi_H = 1$. All the test units are divided into three groups allocated at ξ_H , ξ_L , and ξ_M , respectively, where the middle level of stress is $\xi_M = (\xi_L + \xi_H)/2$. We assume, as is the case in most applications, that the three groups are tested simultaneously until a common censoring time η . With practical values of the planning values, if one does not use the kind of constraint suggested here (and in previous work with compromise ALT test plans), optimization results in an ALT plan with only two levels of stress (the optimum proportion at the middle level would approach zero or the optimum location of the middle level would approach one of the other two levels).

Constant-stress three-level compromise test plans can have a variety of forms. For example, Meeker and Escobar (see, Chapter 20 of [8]) suggest a compromise test plan with a fixed allocation proportion of 0.2 at ξ_M . In this paper, we modify this compromise test plan in the following way. Instead of a fixed π_M , the allocations π_L and π_M at ξ_L and ξ_M , respectively, are chosen such that the expected numbers of failures at ξ_L and ξ_M are equal. This modified compromise test plan is more appropriate for small sample sizes because it does a better job of controlling the probability of having zero failures at the lower stress levels. Under this constraint we choose ξ_L^{opt} and π_L^{opt} to obtain the optimized compromise test plan that minimizes the variance of the ML estimators of a specific function of the ALT model parameters. For a given compromise test plan, we obtain the exact (other than Monte Carlo error

and conditioning on being able to estimate the model parameters) variances of the ML estimators by simulation and compare them with large-sample approximate variances. Our goal is to find an easy-to-apply method to choose a useful test plan defined by (π_L, ξ_L, n) that has good statistical properties and that can achieve the precision desired by a practitioner.

2.2 Model

Our assumed model corresponds to that used in most previous work in this area, summarized in Chapter 6 of [11] and Chapter 20 of [9]. At any level of the standardized stress ξ , the log failure time Y follows a location-scale distribution with constant σ and a cdf $\Pr(Y \leq y) = \Phi[(y - \mu)/\sigma]$. The location parameter depends on (possibly transformed) stress through the linear relationship $\mu = \gamma_0 + \gamma_1 \xi$, where γ_0 and γ_1 are the regression model parameters. In our example, $\Phi(z) = \Phi_{\text{sev}}(z) = 1 - \exp[-\exp(z)]$ is the standardized smallest extreme value distribution corresponding to a Weibull failure time distribution. The failure probabilities at the highest stress and the use stress are $p_H = \Phi[(\log(\eta) - \gamma_0 - \gamma_1)/\sigma]$ and $p_U = \Phi[(\log(\eta) - \gamma_0)/\sigma]$, respectively. It is easy to express the probability at any other stress level ξ as a function of p_U and p_H . Given p_H , p_U , σ and η , one can easily calculate γ_0 and γ_1 .

2.3 ML Estimation

Let $\hat{\gamma}_0$, $\hat{\gamma}_1$ and $\hat{\sigma}$ denote the ML estimators of γ_0 , γ_1 , and σ , respectively. Then the ML estimator of the p quantile at stress level ξ can be expressed as $\hat{y}_p = \hat{\gamma}_0 + \hat{\gamma}_1 \xi + z_p \hat{\sigma}$, where $z_p = \Phi^{-1}(p)$. The large-sample approximate variance of \hat{y}_p is $\text{Avar}(\hat{y}_p) = (1, \xi, z_p) \Sigma_{\hat{\gamma}_0, \hat{\gamma}_1, \hat{\sigma}}(1, \xi, z_p)$, where $\Sigma_{\hat{\gamma}_0, \hat{\gamma}_1, \hat{\sigma}}$ is the large-sample approximate variance-covariance matrix obtained from the inverse of the Fisher information matrix, and the superscript

^T indicates vector transpose (for details on how to do the computations, see, for example, Chapter 20 of Meeker and Escobar [9]). As is common practice in the ALT planning literature, one can compare the relative efficiency of test plans with different samples sizes using the scaled large-sample approximate variance denoted by $(n/\sigma^2)Avar(\hat{y}_p)$. For small sample sizes, however, the scaled variance of \hat{y}_p denoted by $(n/\sigma^2)Var(\hat{y}_p)$ can be obtained to a much higher degree of approximation by using the Monte Carlos simulation, as described in detail in Section 2.4.

2.4 Zero failure problems

In ALTs with a fixed censoring time and small sample sizes, it is possible to have zero failures at one or more levels of stress at the end of the test. An ALT having zero failures at one or more levels of stress would generally be considered to be an unsuccessful ALT. Having zero failure at one or more levels of stress causes the loss of the advantages of a three-level test plan such as the ability to detect a departure from the assumed relationship between life and stress. We refer to this problem as the first type of zero failure problem (ZFP1). Having zero failures at two or more of the three levels of stress will make it impossible to estimate the model parameters or the quantile of interest. We refer to this problem as the second type of zero failure problem (ZFP2).

The s-bias and variance of \hat{y}_p can be obtained via simulations in the following way. Based on the specified planning values, one can simulate sample ALT data. For each simulated data set, one can calculate the ML estimators $\hat{\gamma}_0$, $\hat{\gamma}_1$, and $\hat{\sigma}$ and \hat{y}_p . Using a large number of Monte-Carlo simulations, one can estimate $E(\hat{y}_p)$ and $Var(\hat{y}_p)$, conditional on no ZFP2 (because when a ZFP2 problem arises in a simulation trial estimation of the model parameters is not possible). Our simulation-based evaluations of $Var(\hat{y}_p)$ are conditional on not having a

ZFP2 [and thus, as we will see in our evaluations, such conditional variances could be misleading when $\Pr(\text{ZFP2})$ is not negligible].

Generally, we want to find a test plan that has a small probability of having a ZFP1. Let n_L , n_M and $n_H = n - n_L - n_M$ be the number of test units allocated at ξ_L , ξ_M and ξ_H , respectively and let π_i denote the allocation at stress level ξ_i where $i = L, M$ and H . The number of test units allocated to stress level i is $n_i = \lceil \pi_i n \rceil$, where n is the total sample size and $\lceil \cdot \rceil$ means the rounding to the nearest integer, because $\pi_i n$ may not be an integer. The probability of failing at ξ_i is

$$p_i = \Phi\left(\frac{\log(\eta) - \gamma_0 - \gamma_1 \xi_i}{\sigma}\right). \quad (1)$$

The relationship between π_L and π_M in our compromise test plan is $\pi_L p_L = \pi_M p_M$, which implies an equal expected number of failures at ξ_L and ξ_M . Because all the test units are s-independent, the probability of having zero failures at ξ_i can be expressed as

$$P_i = (1 - p_i)^{n_i}, \quad (2)$$

where $i = L, M$ and H . Thus the probability of ZFP1 is

$$\Pr(\text{ZFP1}) = P_H + P_M + P_L - P_H P_L - P_M P_L - P_M P_H + P_H P_M P_L. \quad (3)$$

Similarly, the probability of ZFP2 can be expressed as

$$\Pr(\text{ZFP2}) = P_H P_L + P_M P_L + P_M P_H - P_H P_M P_L \quad (4)$$

Given the levels of stress, the allocation corresponding to equal expected number of failures at each of the three stress levels π_i^E can be calculated by the following formulas

$$\pi_L^E = \frac{P_H P_M}{P_L P_M + P_M P_H + P_H P_L} \quad (5)$$

$$\pi_M^E = \frac{P_H P_L}{P_L P_M + P_M P_H + P_H P_L} \quad (6)$$

$$\pi_H^E = \frac{P_M P_L}{P_L P_M + P_M P_H + P_H P_L}. \quad (7)$$

Given the three allocations, one can also calculate the lowest and middle levels of stress, ξ_L^E and ξ_M^E , to have an equal expected number of failures at each of the three levels of stress. This can be done by noting that P_i , $i = L, M$ and H depend on the ξ_i values and thus one can solve the following equations for ξ_L^E and ξ_M^E :

$$\pi_H P_H = \pi_M P_M \quad (8)$$

$$\pi_M P_M = \pi_L P_L \quad (9)$$

Using (8) and the relationships (1) and (2), one can obtain ξ_M^E and ξ_L^E from (9).

From (3), one can obtain π_L^S , a value of π_L to minimize $\Pr(\text{ZFP1})$. However, we do not have a simple analytical expression of π_L^S for given p_L , p_H and n . In practice, as is shown in Section 3.3, π_L^S is close to and a little larger than π_L^E . Because π_i^E $i = L, M$ and H do not depend on the sample sizes, using π_i^E can make the following test plan specification and evaluation simpler than using π_L^S .

2.5 The adhesive-bond ALT example and planning values

To illustrate the ideas presented in this paper, we will use the adhesive-bond test-planning example that was described in [7] and on page 535 of [9]. In this example, the Weibull-distribution planning values were given as $p_H = 0.9$, $p_U = 0.001$, and $\sigma = 0.6$, based on previous experience with similar products. The censoring time is $\eta = 183$ days. The quantity of interest is the 0.1 quantile (i.e., $p = 0.1$) of the failure-time distribution at the use stress level of 50 °C. Using the above planning values, we obtain $\gamma_0 = 9.35$, $\gamma_1 = -4.64$ and $y_{0.1} = 8.0$ by using the formulas in Section 2.2. In the Meeker and Escobar [9] example, 300 units were available for testing. Here we will investigate test plans with fewer than 300 test units.

We will also assume there is uncertainty in the planning values. To do this we will evaluate the compromise test plan properties using alternative planning values. In Section 4.2 we show that when considering misspecification of the three planning values for the parameters over the range of a cube, it is sufficient to do one further evaluation at one of the corners of the cube.

We call the planning values at this corner of the cube the *critical point planning values* or CPPV. For our example the CPPV is $p_H = 0.45$, $p_U = 0.0005$ and $\sigma = 0.75$.

3 Evaluation of Optimized Compromise Test Plan with Small Samples

3.1 Zero failure problems of a previous compromise test plan

It is important to investigate the zero-failure behavior of the compromise test plans such as those with a fixed π_M proposed in [6] and [9]. Fixing $\pi_M = 0.2$, one can obtain an optimized (i.e., minimum $\text{Avar}(\hat{y}_{0.1})$) compromise test plan by choosing $\pi_L = 0.531$ and $\xi_L = 0.638$ under planning values $p_H = 0.9$, $p_U = 0.001$, and $\sigma = 0.6$. Figure 1 shows the probabilities of both ZFP1 (dotted line) and ZFP2 (solid line) as a function of n when $\pi_L = 0.531$ and $\xi_L = 0.638$ for two points of planning values: $p_H = 0.9$, $p_U = 0.001$ and $\sigma = 0.6$ (on the left) and $p_H = 0.45$, $p_U = 0.0005$ and $\sigma = 0.75$ (on the right).

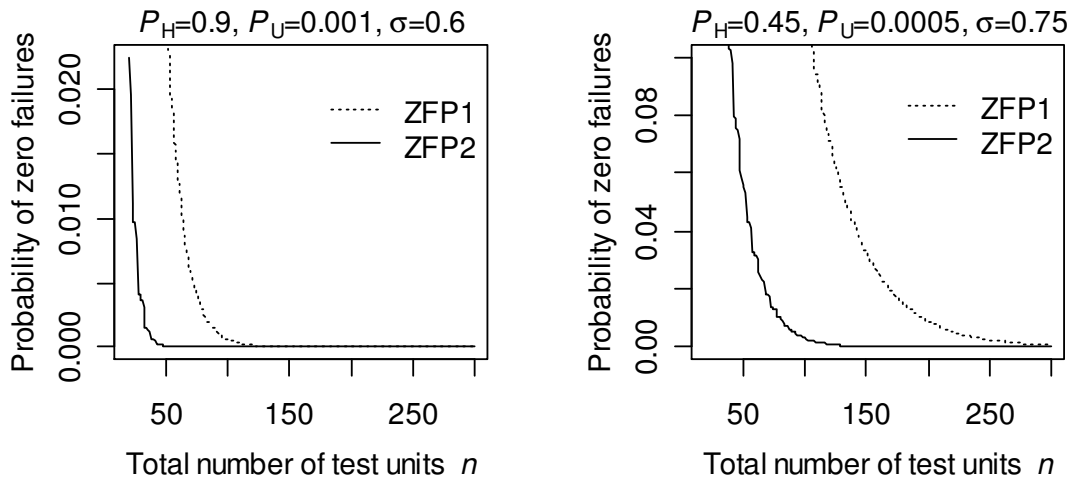


Figure 1: $\Pr(\text{ZFP1})$ (dotted line) and $\Pr(\text{ZFP2})$ (solid line) as a function of n when $\pi_L = 0.531$ and $\xi_L = 0.638$ for two sets of planning value (i) the original planning values: $p_H = 0.9$, $p_U = 0.001$ and $\sigma = 0.6$ (on the left) and (ii) the CPPV: $p_H = 0.45$, $p_U = 0.0005$ and $\sigma = 0.75$ (on the right).

Figure 1 shows that $\Pr(\text{ZFP1})$ is much higher than $\Pr(\text{ZFP2})$. This is because there are many more events leading to ZFP1 than ZFP2. Figure 1 also shows that the probabilities of having ZFP1 or ZFP2 under CPPV are much higher than the corresponding probabilities under the original planning values. Thus, it is important to consider the zero failure probabilities under both the original planning values and the corresponding CPPV.

To further investigate the cause of ZFP1 in Figure 1, consider $P_{LM} = P_L + P_M - P_L P_M$, the probability of having zero failures at either ξ_L or ξ_M regardless of the number of failures at ξ_H . If one plots P_{LM} versus n on Figure 1, the curve would be indistinguishable from the curve of $\Pr(\text{ZFP1})$ versus n in Figure 1. Thus ZFP1 is caused, primarily, by having no failures at either ξ_L or ξ_M . To assure that there are failures at both ξ_L and ξ_M , practitioners should control $\Pr(\text{ZFP1})$ to be below some specified small value, say, 0.01.

It is possible that an optimized compromise test plan with π_M other than 0.2 may have a smaller probability of ZFP1 than that for $\pi_M = 0.2$. For each value of π_M , there is a corresponding optimized compromise test plan and a probability of ZFP1 associated with the plan. Figure 2 shows $\Pr(\text{ZFP1})$ of those optimized compromise test plans as a function of π_M for $n = 40, 60$ and 90 and the original planning values (on the left) and the CPPV (on the right). The vertical dotted lines indicate the values of π_M that result in having an equal expected number of failures at ξ_L and ξ_M . The zigzag behavior comes from the integer sample-size rounding effect described in Section 2.4.

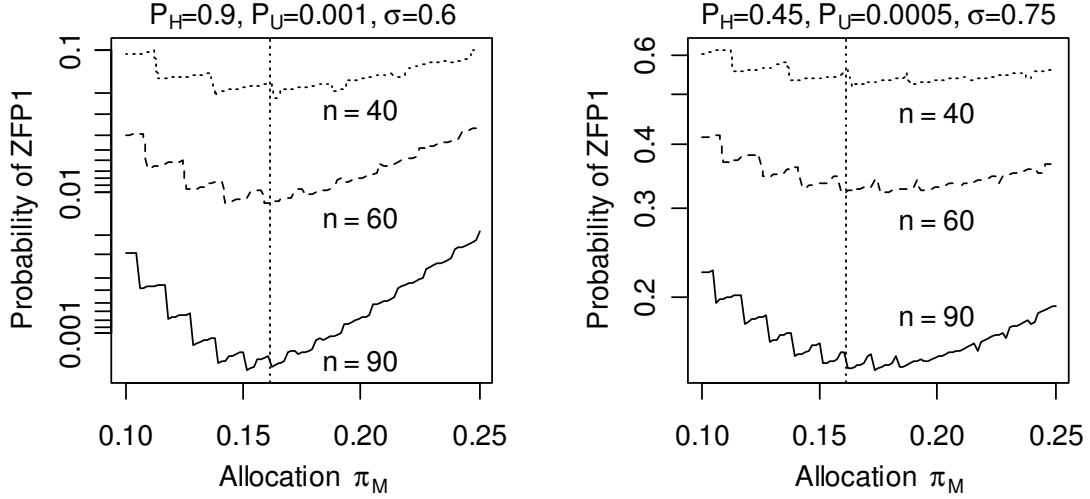


Figure 2: Pr(ZFP1) of optimized compromise test plans as a function of π_M for $n = 40, 60$ and 90 and two sets of planning values: (i) the original planning values ($p_H = 0.9, p_U = 0.001$ and $\sigma = 0.6$) on the left and (ii) the CPPV ($p_H = 0.45, p_U = 0.0005$ and $\sigma = 0.75$) on the right. The vertical dotted lines show the value of π_M at which the expected numbers of failures at ξ_L and ξ_M are equal.

Figure 2 shows that there is a value of π_M at which $\Pr(\text{ZFP1})$ is minimum for a specific sample size. The value of π_M is close to that of an optimized compromise test plan with an equal expected number of failures at ξ_L and ξ_M [i.e., (9) holds]. Thus, to achieve, in a simple way, a small ZFP1 probability when the sample sizes are small, we suggest using a compromise test plan with an equal expected numbers of failures at ξ_L and ξ_M . In the remainder of this paper, the term compromise test plans refers only to the compromise test plans with an equal expected number of failure at ξ_L and ξ_M .

3.2 Adequacy of the large-sample approximate variance

Figure 3 shows the scaled actual variance $(n/\sigma^2)\text{Var}(\hat{y}_{0.1})$ conditional on no ZFP2 (on the left) and the corresponding $\Pr(\text{ZFP1})$ (on the right) as a function of the total sample size n , under the different planning values and test plans. The horizontal lines on the left plots show $(n/\sigma^2)\text{Avar}(\hat{y}_{0.1})$. The actual variances were obtained by using Monte-Carlo simulations with

data generated from the compromise test plan with an equal expected failure number at ξ_L and ξ_M described in Section 3.1. These figures provide an assessment of the adequacy of the large sample approximation for $(n/\sigma^2)\text{Var}(\hat{y}_{0.1})$ and we can see when the approximation may be inadequate when n is too small.

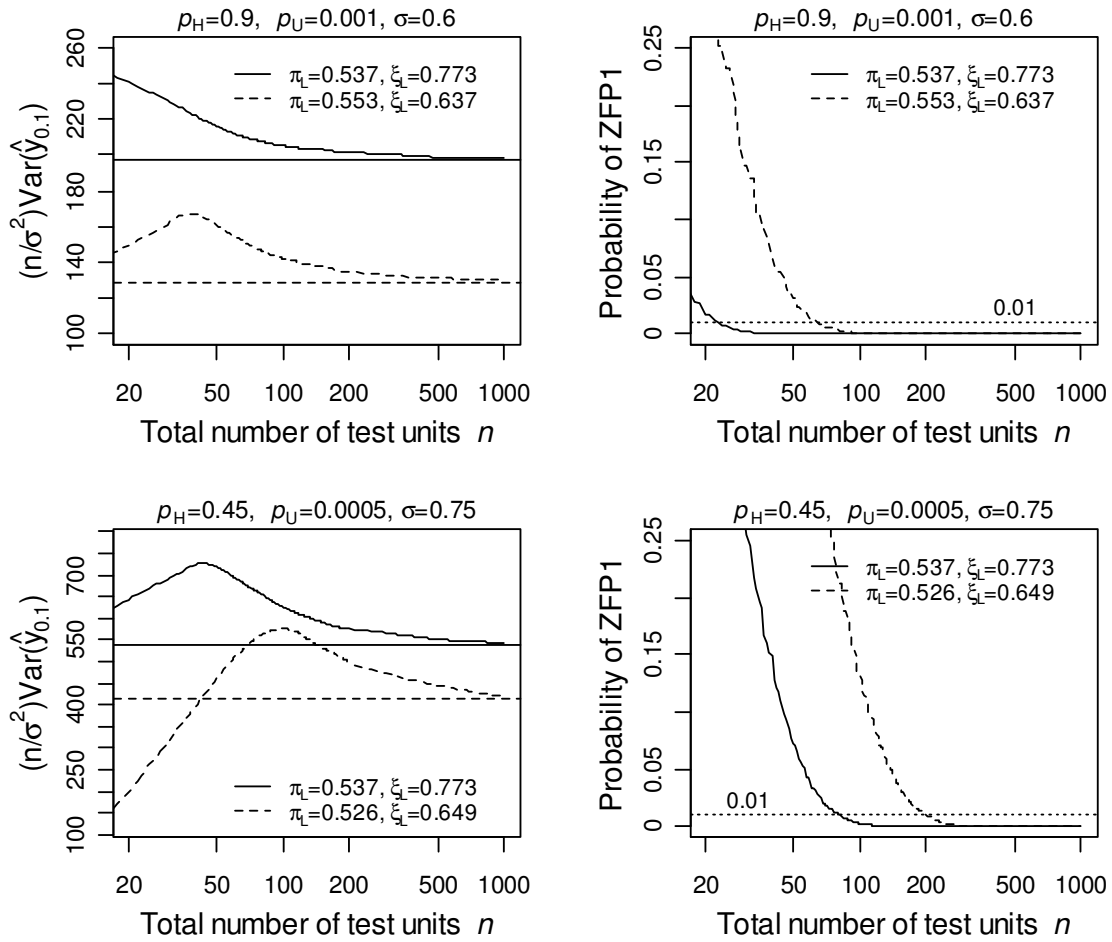


Figure 3: The plots on the left side are the smoothed scaled variances $(n/\sigma^2)\text{Var}(\hat{y}_{0.1})$, conditional on no ZFP2 as a function of n under original planning values (top) and the CPPV (bottom). The horizontal lines show the corresponding $(n/\sigma^2)\text{Avar}(\hat{y}_{0.1})$. The simulated curves are based on 10,000 simulations at each point using the Weibull distribution model under the compromise three-level constant-stress test plans with an equal expected number of failures at ξ_L and ξ_M . The plots on the right side show the corresponding $\Pr(\text{ZFP1})$ calculated by using (3). The dotted horizontal lines indicate where $\Pr(\text{ZFP1}) = 0.01$.

Figure 3 shows for the original planning values (top) and the CPPV (bottom), the optimized [i.e., the minimum $\text{Avar}(\hat{y}_{0.1})$] compromise test plans obtained by adjusting π_L and ξ_L . For the original planning values, the optimized compromise test plan has $\pi_L = 0.553$ and $\xi_L = 0.637$. For the CPPV planning values, the optimized compromise test plan has $\pi_L = 0.526$ and $\xi_L = 0.649$. As expected, given the same planning values and number of test units, compared with the non-optimized test plans, the optimized test plans provide smaller variances at the expense of a higher probability of ZFP1.

Another important observation from Figure 3 is that $(n/\sigma^2)\text{Var}(\hat{y}_{0.1})$, conditional on no ZFP2, first increases with n until a maximum value and then decreases, approaching $(n/\sigma^2)\text{Avar}(\hat{y}_{0.1})$ for large n . The maximum value of $(n/\sigma^2)\text{Var}(\hat{y}_{0.1})$ can be as high as around 40% larger than $(n/\sigma^2)\text{Avar}(\hat{y}_{0.1})$. The maximum value occurs when the probability of ZFP2 is between 0.01 and 0.02. The reason for this phenomenon is that when $\text{ZFP2} < 0.01$, the probability of ZFP2 decreases rapidly with n , resulting in less conditioning and a more accurate representation of the true (unconditional) sample variability.

3.3 Reduction of the risk of ZFP1

Figure 4 shows $\text{Pr}(\text{ZFP1})$ as a function of the allocation π_L (left) or ξ_L (right) when $\xi_L = 0.637$ or $\pi_L = 0.553$, respectively. These probabilities were computed from the original planning values. Again, the zigzag behavior comes from the integer sample-size rounding effect described in Section 2.4.

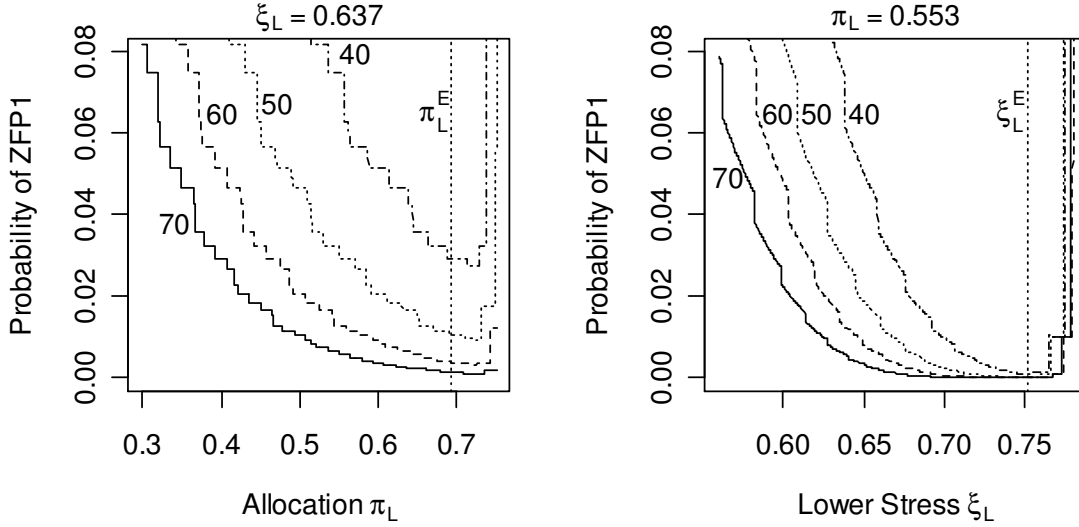


Figure 4: $\Pr(\text{ZFP1})$ as a function of the unit allocation π_L (left) and the lowest level of stress ξ_L (right) at $\xi_L = 0.637$ or $\pi_L = 0.553$, respectively, for $n = 40, 50, 60$, and 70 with the original planning values $p_H = 0.9$, $p_U = 0.001$, and $\sigma = 0.6$. The dotted vertical lines correspond to $\pi_L^E = 0.692$ and $\xi_L^E = 0.752$, respectively.

In Figure 4, the left-hand plot shows that when π_L increases from $\pi_L = 0.3$, $\Pr(\text{ZFP1})$ (primarily occurring at ξ_L or ξ_M in this situation) decreases until $\pi_L \approx \pi_L^E$. When π_L increases beyond π_L^E a value obtained from (5), $\Pr(\text{ZFP1})$ (primarily occurring at ξ_H) will ultimately increase. The right-hand plot in Figure 4 shows that when ξ_L increases beyond $\xi_L = 0.56$, $\Pr(\text{ZFP1})$ (primarily occurring at ξ_L or ξ_M in this situation) decreases until $\xi_L \approx \xi_L^E$, [where ξ_L^E is obtained by solving (8) and (9)]. When ξ_L increases beyond ξ_L^E , $\Pr(\text{ZFP1})$ (primarily occurring at ξ_H) will, again, ultimately increase. To have more precise estimation with small sample sizes while controlling $\Pr(\text{ZFP1})$ to be small, we suggest selecting π_L or ξ_L to be smaller than or close to π_L^E or ξ_L^E , respectively.

3.4 Evaluating the compromise test plan

It is interesting to examine the relationship between the simulated actual variance and the large sample approximate variance under the compromise test plans for finite sample sizes. We can compare the scaled variance of ML estimators as functions of π_L or ξ_L around the point

($\pi_L^{Opt} = 0.553$, $\xi_L^{Opt} = 0.637$), corresponding to the large-sample approximate optimized compromise test plan for the original planning values $p_H = 0.9$, $p_U = 0.001$, and $\sigma = 0.6$. Figure 5 shows $(n/\sigma^2)\text{Var}(\hat{y}_{0.1})$ (solid and dotted curves) conditional on no ZFP2 and $(n/\sigma^2)\text{Avar}(\hat{y}_{0.1})$ (dashed curves), both as a function of the allocation π_L with four different values of n and a fixed ξ_L . The parts of the curves with dotted lines in Figure 5 represent the values of π_L where $\text{Pr}(\text{ZFP1}) \geq 0.01$. The $(n/\sigma^2)\text{Avar}(\hat{y}_{0.1})$ curves are, of course, the same for all sample sizes. The two vertical dotted lines represent π_L^{Opt} (on the left) and π_L^E (on the right). These allocations can be calculated directly from (5), (8), and (9).

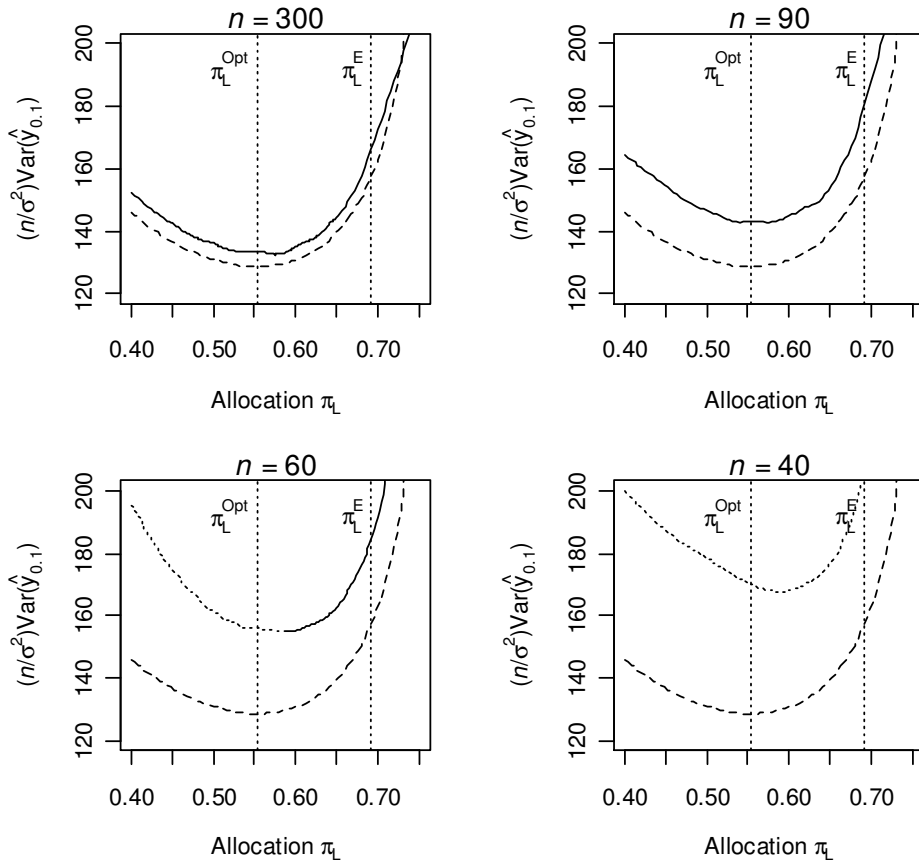


Figure 5: Smoothed $(n/\sigma^2)\text{Var}(\hat{y}_{0.1})$ conditional on no ZFP2 and $(n/\sigma^2)\text{Avar}(\hat{y}_{0.1})$ for the Weibull distribution failure-time model as a function of the allocation π_L based on 10,000 simulations at each point

with $\xi_L = 0.637$ and the original planning values. The dashed lines show $(n/\sigma^2)A\text{var}(\hat{y}_{0.1})$. The two vertical dotted lines represent π_L^{Opt} and π_L^E , respectively. The dotted parts of the smoothed curves correspond to the values of π_L where $\text{Pr}(\text{ZFP1}) \geq 0.01$.

The simulated $(n/\sigma^2) \text{Var}(\hat{y}_{0.1})$ is larger than the large-sample approximate $(n/\sigma^2)A\text{var}(\hat{y}_{0.1})$. When $n = 300, 90,$ and 60 the minimum $(n/\sigma^2) \text{Var}(\hat{y}_{0.1})$ occurs at a value of π_L close to π_L^{Opt} [based on minimizing $(n/\sigma^2)A\text{var}(\hat{y}_{0.1})$]. For $n = 40$ the minimum scaled variance is importantly larger than π_L^{Opt} . These results suggest that even when $A\text{var}(\hat{y}_p)$ does not provide a good approximation for $\text{Var}(\hat{y}_p)$, it can provide a good approximation for minimizing $(n/\sigma^2) \text{Var}(\hat{y}_{0.1})$ as long as $\text{Pr}(\text{ZFP1})$ is not too large.

Another observation from Figure 5 is that, in the vicinity of π_L^E , $(n/\sigma^2) \text{Var}(\hat{y}_{0.1})$ is smaller when $\pi_L < \pi_L^E$ than when $\pi_L > \pi_L^E$. When $\pi_L < \pi_L^E$, $\text{Pr}(\text{ZFP1})$ due to no failures at ξ_L or ξ_M is higher than that at ξ_H . When $\pi_L > \pi_L^E$, $\text{Pr}(\text{ZFP1})$ due to no failures at ξ_H is higher than that at ξ_L or ξ_M . Because there is a distinct increase in $(n/\sigma^2) \text{Var}(\hat{y}_{0.1})$ at π_L^E when compared to that at π_L^{Opt} , as long as a specific criterion for the risk of ZFP1, say, $\text{Pr}(\text{ZFP1}) \leq 0.01$, is satisfied, one should select a $\pi_L < \pi_L^E$ to reduce $(n/\sigma^2) \text{Var}(\hat{y}_{0.1})$.

Figure 6 is similar to Figure 5, showing $(n/\sigma^2) \text{Var}(\hat{y}_{0.1})$ and $(n/\sigma^2)A\text{var}(\hat{y}_{0.1})$ as a function of ξ_L with four different values of n and a fixed value of π_L . Again, the dotted parts of the curves show where $\text{Pr}(\text{ZFP1}) \geq 0.01$. The two vertical dotted lines indicate the location of ξ_L^{Opt} and ξ_L^E .

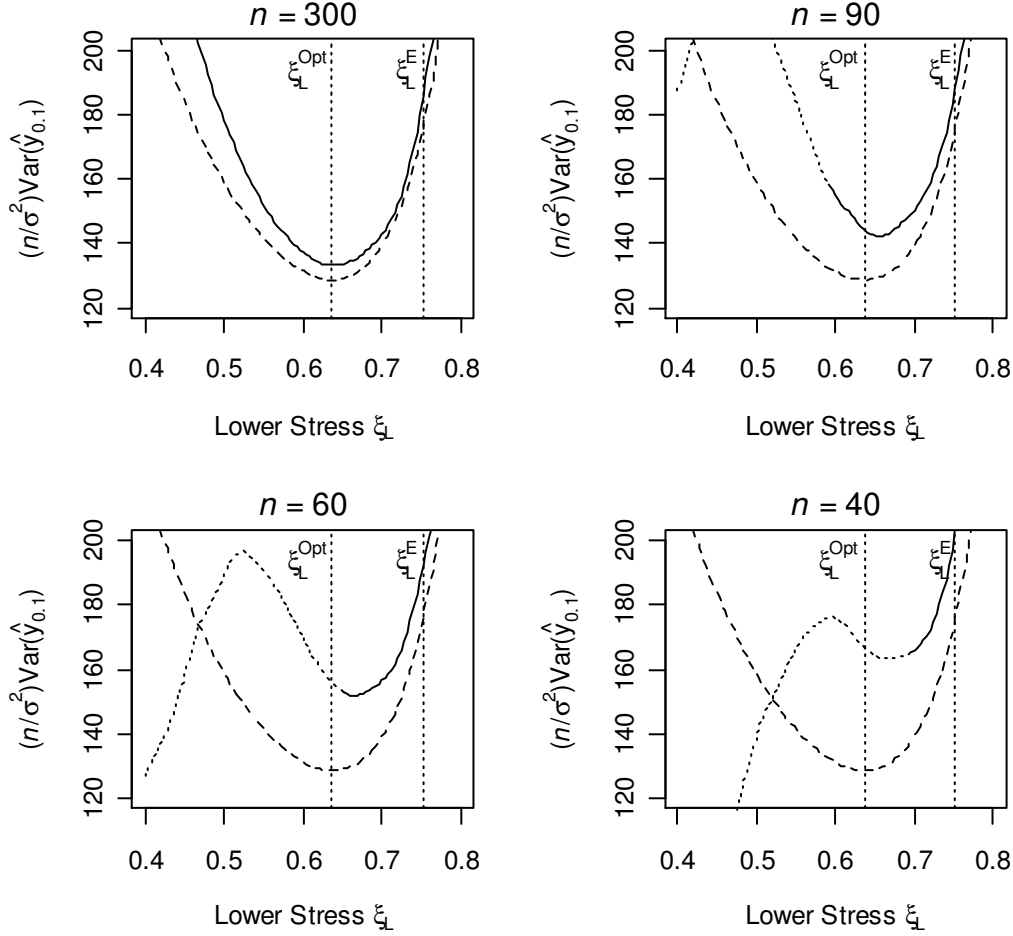


Figure 6: Smoothed $(n/\sigma^2)\text{Var}(\hat{y}_{0.1})$ conditional on no ZFP2 for the 0.1 quantile (solid or dotted curves) of the Weibull failure distribution as a function of the lowest level of stress ξ_L from 10,000 simulations in each point with $\pi_L = 0.553$ and the planning values $p_H = 0.9$, $p_U = 0.001$ and $\sigma = 0.6$. The dashed lines represent $(n/\sigma^2)\text{Avar}(\hat{y}_{0.1})$. The two vertical dashed lines represent ξ_L^{Opt} (the left) and ξ_L^E (the right). The dotted parts of the curves correspond to values of ξ_L where $\text{Pr}(\text{ZFP1})$ is larger than 0.01.

When $n = 300$, the minimum $(n/\sigma^2)\text{Var}(\hat{y}_{0.1})$ occurs very close to ξ_L^{Opt} , the optimized lowest level of stress under the large-sample approximation. Note, however, that $(n/\sigma^2)\text{Var}(\hat{y}_{0.1})$ is always larger than $(n/\sigma^2)\text{Avar}(\hat{y}_{0.1})$ for $n = 300$. When $n = 90$, the simulated scaled variance (the dotted line) is increasing in ξ_L when $\xi_L < 0.45$. When $\xi_L > 0.5$, $(n/\sigma^2)\text{Var}(\hat{y}_{0.1})$ decreases in ξ_L until it reaches a minimum, after which it increases. When $n = 60$ or 40, the conditional $(n/\sigma^2)\text{Var}(\hat{y}_{0.1})$ is increasing in ξ_L when ξ_L is small and then is decreasing as ξ_L increases

after a turning point. At the turning point the probability of ZFP2 is between 0.01 and 0.02, similar to the phenomenon described in Section 3.2. When ξ_L becomes larger, after passing through a minimum point, $(n/\sigma^2) \text{Var}(\hat{y}_{0.1})$ is increasing in ξ_L again. The values of ξ_L at the minimum point are a little larger than ξ_L^{Opt} . Note that the small values of the conditional $(n/\sigma^2) \text{Var}(\hat{y}_{0.1})$ are of little use when the probability of ZFP2 is importantly large (say greater than 0.01).

Another observation from Figure 6 is that, in the vicinity of ξ_L^E , $(n/\sigma^2) \text{Var}(\hat{y}_{0.1})$ is smaller when $\xi_L < \xi_L^E$ than when $\xi_L > \xi_L^E$. When $\xi_L < \xi_L^E$, $\text{Pr}(\text{ZFP1})$ is higher at ξ_L and ξ_M . When $\xi_L > \xi_L^E$, $\text{Pr}(\text{ZFP1})$ is higher at ξ_H . Because there is an important increase of the variance at ξ_L^E when compared to that at ξ_L^{Opt} , as long as a specific criterion to the risk of ZFP1 say, $\text{Pr}(\text{ZFP1}) \leq 0.01$, is satisfied, one should select a $\xi_L < \xi_L^E$ to reduce the variance.

Figures 5 and 6 show that, when $\text{Pr}(\text{ZFP1}) \leq 0.01$, although $(n/\sigma^2) \text{Var}(\hat{y}_{0.1}) \geq (n/\sigma^2) \text{Avar}(\hat{y}_{0.1})$, their minimum points in term of (π_L, ξ_L) for different values of n are close to each other. This implies that the easy-to-compute $(n/\sigma^2) \text{Avar}(\hat{y}_{0.1})$ can be used as a guide to find an initial test plan.

Based on the information given in Section 3, we use the following strategy to find a useful ALT plan.

1. Use the simple analytical formulas in Section 2.4 to determine the region of (π_L, ξ_L, n) in which $\text{Pr}(\text{ZFP1})$ is below the practitioner's ZFP1 critical level (say 0.01).
2. Minimize $(n/\sigma^2) \text{Avar}(\hat{y}_p)$, subject to the constraint that $\text{Pr}(\text{ZFP1})$ is less than the ZFP1 critical level, to obtain a tentative test plan.
3. Run simulations in the region of the tentative plan to fine tune the choice of π_L and ξ_L and to get the value of the actual variance for the test plan.

4 Test Plan Selection

4.1 Test plan properties for given planning values

Figure 7 is a contour plot showing $(n/\sigma^2)Avar(\hat{y}_{0.1})$ and $\Pr(\text{ZFP1})$ as a function of ξ_L and π_L using the compromise three-level test plan described in Section 3.4. The contours show $(n/\sigma^2)Avar(\hat{y}_{0.1})$ and the zigzag parallel lines show $\Pr(\text{ZFP1})$ for different sample sizes. Again, the zigzag behavior comes from the integer sample-size rounding effect described in Section 2.4. The solid line labeled $\pi_L^E \sim \xi_L^E$ shows where there is an equal expected number of failures at ξ_L and ξ_H . This line can be obtained by plotting π_L^E as a function of ξ_L , or equivalently by plotting ξ_L^E as a function of π_L . The region below this line is where we will find a useful test plan.

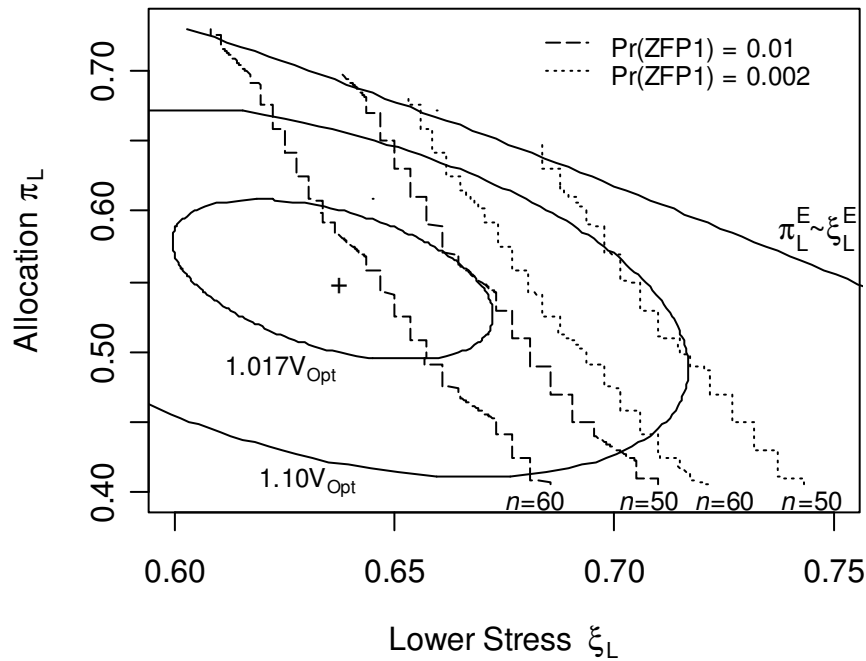


Figure 7: Contour plot showing $(n/\sigma^2)Avar(\hat{y}_{0.1})$ and ZFP1 for the Weibull distribution model and the original planning values. The symbol “+” at the point $(\pi_L = 0.553, \xi_L = 0.637)$ indicates the location of the minimum $(n/\sigma^2)Avar(\hat{y}_{0.1}) = V_{\text{Opt}} = 128.7$. The zigzag parallel lines correspond to particular values of

Pr(ZFP1) (the dashed: 0.01 and the dotted: 0.002) for $n = 50$ and 60 , respectively. The solid line labeled $\pi_L^E \sim \xi_L^E$ shows where the expected numbers of failures at ξ_L and ξ_H are equal.

Figure 7 illustrates the simple strategy to find a test plan. First, one can draw several zigzag lines representing a small ZFP1 probability, say 0.01, for different sample sizes. Then, draw the contours of the scaled large-sample approximate variance. Along a zigzag line (corresponding to a sample size and a ZPF1 constraint), a point that is close to a contour is a suitable candidate for the desired test plan having the smallest $\text{Avar}(\hat{y}_p)$ for a specified sample size and small ZFP1 probability. Considering different zigzag lines, one can evaluate the tradeoff between sample size and $\text{Pr}(\text{ZFP1})$ to get the desired precision.

4.2 Test planning with uncertain of planning values

Because there is always some degree of misspecification in the planning values, it is important to check the impact that the uncertainty of planning values will have on the variance, the ZFP1 probability and the choice of test plan for small sample sizes. For the adhesive-bond example, if the practitioner is confident that the true values of p_H , p_U , and σ are in the intervals (0.45, 0.95), (0.0005, 0.0015), and (0.45, 0.75), respectively, based on previous experience, separate contour plots could be made for each combination and these could be used to find a plan that is satisfactory over the region of planning value uncertainty.

Suppose that the ranges of the planning-values uncertainty can be described by a cube containing all possible true values of (p_H, p_U, σ) . There are eight corners in the cube. Note that $\text{Avar}(\hat{y}_p)$ increases as σ increases and as p_H or p_U decreases, and the ZFP1 probability increases as p_H or p_U decreases. Therefore, the corner with the smallest p_H and p_U and the largest σ represents the largest possible values of both variance and the ZFP1 probability simultaneously. As described in Section 2.5, we refer to this combination as the critical planning

value point (CPPV), because once the variance and $\Pr(\text{ZFP1})$ at this set meet certain requirements, these requirements will be satisfied automatically throughout the entire cube. Thus, it is sufficient to investigate this critical point to evaluate the maximum impact of the incorrect planning values.

Figure 8 illustrates our procedure to find a good starting ALT test plan.

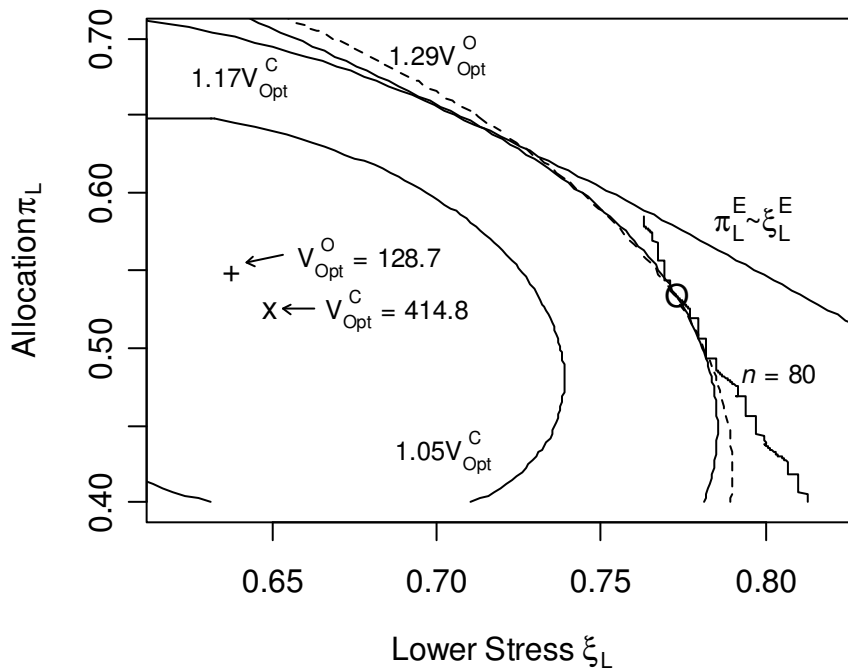


Figure 8: Contour plots illustrating the procedure to find a good starting ALT test plan (details in the text).

The contours in Figure 8 show $(n/\sigma^2)\text{Avar}(\hat{y}_{0,1})$, relative to the value at minimum, when the true parameters are equal to the CPPV (solid lines) and the original planning values (dashed line). The “x” point indicates the position of the minimum point $\pi_L = 0.526$ and $\xi_L = 0.649$ where $(n/\sigma^2)\text{Avar}(\hat{y}_{0,1}) = 414.8$ when the true parameters are equal to the CPPV. The “+” point indicates, as in Figure 7, the position of the minimum when the true parameters are equal to the

original planning values. The solid curve labeled $\pi_L^E \sim \xi_L^E$ shows where there is an equal expected number of failures at ξ_L and ξ_H when the true parameters are equal to the CPPV. The zigzag line is where $\Pr(\text{ZFP1}) = 0.01$ for $n = 80$. The dashed contour represents $(n/\sigma^2) \text{Avar}(\hat{y}_{0.1})$, relative to the minimum when the true parameters are equal to the original planning values. The small circle indicates the point along the zigzag line where $(n/\sigma^2) \text{Avar}(\hat{y}_{0.1})$ is minimized and thus gives the tentative candidate test plan ($\pi_L = 0.537$, $\xi_L = 0.773$ and $n = 80$) when the true parameters are equal to the CPPV, thus taking into consideration the impact of the incorrect planning values. Note that Figure 3 shows $(n/\sigma^2) \text{Var}(\hat{y}_{0.1})$ conditional on no ZFP2 as a function of sample size when the test plans are chosen at the three points “x”, “+” and the small circle.

Suppose that we desire to have $\Pr(\text{ZFP1}) \leq 0.01$ and $\text{Var}(\hat{y}_{0.1}) \leq 4.6$ at the CPPV. At the same time, the sample size should be as small as possible. Computing properties of the test plan at the small circle shows that, under the CPPV, $\text{Avar}(\hat{y}_{0.1}) = 3.76$. From Figure 3, there is roughly a 20% increase from $(n/\sigma^2) \text{Avar}(\hat{y}_{0.1})$ to $(n/\sigma^2) \text{Var}(\hat{y}_{0.1})$ when $n = 80$ and $\Pr(\text{ZFP1}) = 0.01$ under the CPPV. Thus the actual $\text{Var}(\hat{y}_{0.1})$ under the CPPV will be approximately $1.2 \times 3.76 = 4.5$. Therefore, the test plan with $\pi_L = 0.537$, $\xi_L = 0.773$ and $n = 80$ is a candidate that meets our criteria at the CPPV. Using the same test plan with $n = 80$ and assuming that the values of the true parameters p_H , p_U , and σ are equal to the original planning values, we obtain $\text{Var}(\hat{y}_{0.1}) \approx 1.0$ using similar calculations.

4.3 Verification of the candidate test plan

Section 4.2 showed how to find a candidate test plan to control the $\Pr(\text{ZFP1})$ and minimize $(n/\sigma^2) \text{Var}(\hat{y}_{0.1})$. Because there is uncertainty in the adequacy of the large sample approximate variance used in the initial optimization, however, the candidate test plan needs to be verified by more accurate simulations. To do this for the adhesive bond example, we examine the simulated scaled variance around the small circle along the zigzag line in Figure 8.

The solid lines in Figure 9 show the conditional $(n/\sigma^2) \text{Var}(\hat{y}_{0.1})$ as a function of π_L when $n = 80$, corresponding to the point (π_L, ξ_L) on the zigzag line shown in Figure 8. The dashed zigzag curves show $(n/\sigma^2) \text{Avar}(\hat{y}_{0.1})$. The plots on the left (right) are for the situation when the true parameters are equal to the original planning values (equal to the CPPV). The zigzag behavior of the curves is again the result of changing discrete allocations of test units to the stress levels. The location of π_L where the smallest $(n/\sigma^2) \text{Var}(\hat{y}_{0.1})$ occurs under the CPPV is consistent with what is implied by Figure 8. In particular, along the zigzag line in Figure 8, the test plan around the point “O” has the smallest variance under the CPPV. The actual $\text{Var}(\hat{y}_{0.1})$ values are 0.93 and 4.57 under the original planning values and the CPPV, respectively.

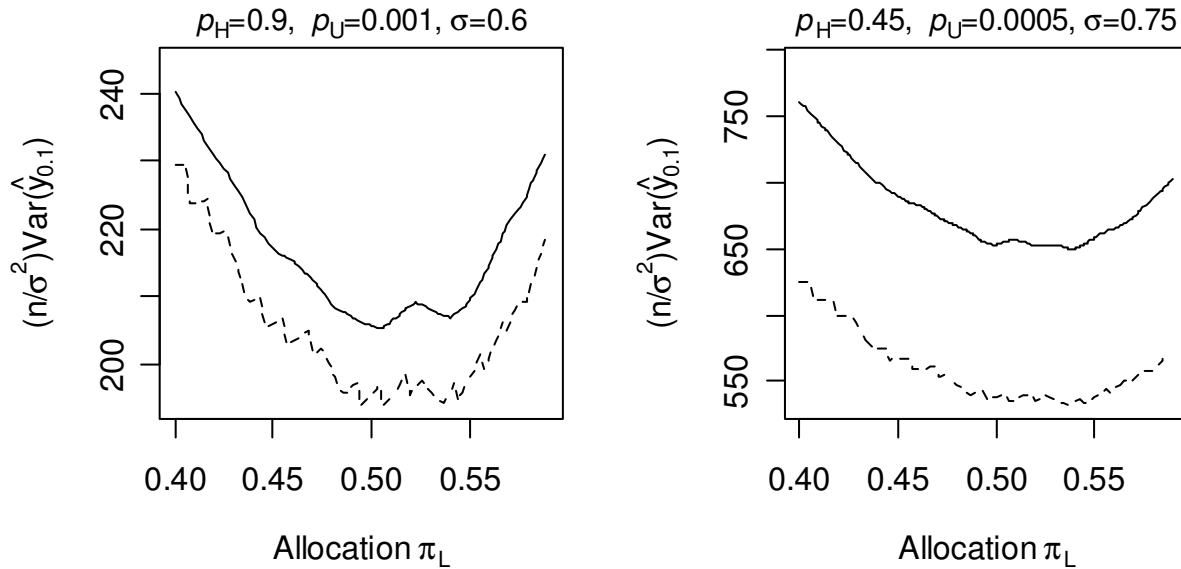


Figure 9: Simulated $(n/\sigma^2) \text{Var}(\hat{y}_{0.1})$ (smoothed solid lines) conditional on no ZFP2 and $(n/\sigma^2) \text{Avar}(\hat{y}_{0.1})$ (dashed lines) for the 0.1 quantile of the Weibull failure distribution as a function of π_L from 10,000 simulations at each point, while the point (π_L, ξ_L) is on the zigzag line shown in Figure 8 where $\text{Pr}(\text{ZFP1}) = 0.01$ with $n = 80$ under the CPPV. The left plot is for the original planning values $p_H = 0.9, p_U = 0.001$ and $\sigma = 0.6$ and the right is for the CPPV $p_H = 0.45, p_U = 0.0005$ and $\sigma = 0.75$.

Figures 8 and 9 illustrate the strategy to select a useful test plan that has a low risk of ZFP1 while achieving the smallest possible variance after considering the uncertainty of planning values. Note that constructing Figure 8 does not need any simulation. Thus this strategy minimizes the number of simulations that are needed and can allow one to find a useful test plan quickly.

Recall that Figure 2 shows that $\Pr(\text{ZFP1})$ for a test plan with an equal expected number of failures at ξ_L and ξ_M is close to but may not be the minimum for a specific sample size due to the zigzag nature of $\Pr(\text{ZFP1})$. Thus, it might be possible to find a slightly better test plan without the constraint of equal expected failure numbers at ξ_L and ξ_M around the small circle.

Finally, we would like to point out that the reason why we only consider the variance and not the s-bias of the quantile estimators is because, under the assumed model, the s-bias contribution to mean square error is negligible compared with variance when we control the risk of ZFP1 to be small.

5 Possible departure from the normal approximation for s-confidence intervals

Normal approximation s-confidence intervals are based on the assumption that the quantity $\hat{z}_p = (\hat{y}_p - y_p) / \sqrt{\text{V}\hat{\text{a}}\text{r}(\hat{y}_p)}$ can be approximated by the standard normal distribution, where $\text{V}\hat{\text{a}}\text{r}(\hat{y}_p)$ is usually the local-information estimator of $\text{Var}(\hat{y}_p)$. We call \hat{z}_p a “t-like” statistic because of its similarity to the t -statistic used in normal-distribution inference. Especially when doing accelerated life testing with a small number of test units, the normal-distribution approximation may be inadequate when the expected number of failures is small. Here we show how to study the possible departure of actual coverage from the normal approximation.

Figure 10 shows normal Q-Q plots of $\hat{z}_{0.1}$ for $n = 80$, obtained from 1,000 simulations from the optimized compromise test plan ($\pi_L = 0.553$, $\xi_L = 0.637$) on the left, and the recommended test plan ($\pi_L = 0.537$, $\xi_L = 0.773$) on the right, for the true parameters $p_H = 0.9$, $p_U = 0.001$, $\sigma = 0.6$ (top), and the true parameters $p_H = 0.45$, $p_U = 0.0005$, $\sigma = 0.75$ (bottom), respectively. These two points in the parameter space correspond to the original planning values and the CPPV. Except for the plot on the NE of Figure 10, all of the plots show departures from the normal distribution in the upper tail. Interestingly, the departures are not too bad in the lower tail for the recommended plans on the NW and SE of Figure 10. Note, however, that a deviation in upper (lower) tail of the t -like statistics will lead to a lower (upper) s -confidence bound with poor coverage properties. In reliability applications, it is usually the lower bound on a quantile that is of most interest.

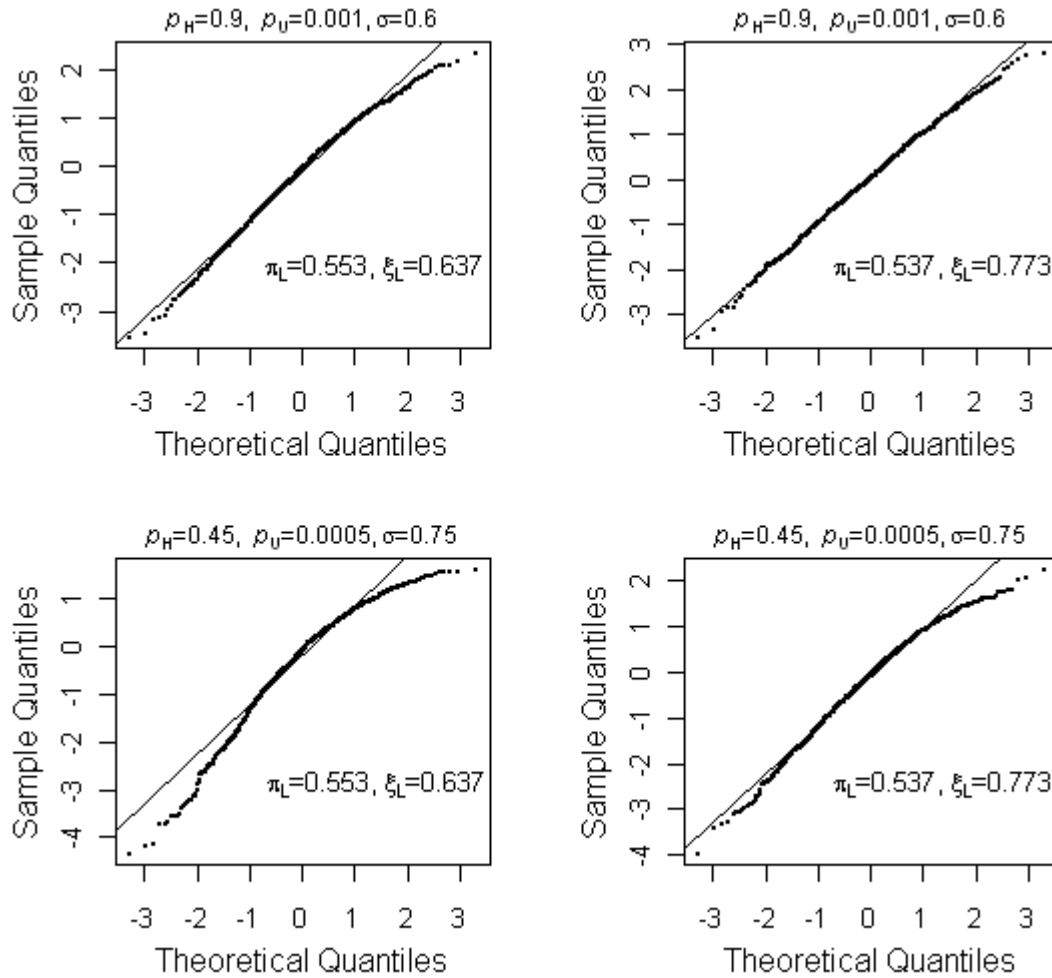


Figure 10: Normal Q-Q plots of $\hat{z}_{0.1}$ the simulated standardized variance conditional on no ZFP2 of the 0.1 quantile of the Weibull failure time distribution for $n = 80$, obtained from 1,000 simulations at test plans $(\pi_L = 0.553, \xi_L = 0.637)$ on the left and $(\pi_L = 0.537, \xi_L = 0.773)$ on the right for the true parameters to be the original planning values (top) and the CPPV (bottom), respectively.

Table 1 shows the expected number failing at each test condition for each combination of test plan and planning values. As suggested by Table 1, the normal approximation tends to be especially poor when the expected number of failures at the individual test conditions is small. These results suggest that when the expected number of failures is small, one should use better confidence interval procedures such as those based on the bootstrap (see for example [4]) or the

inversion of a likelihood ratio test (see for example [14]) to have a procedure with a more accurate coverage probabilities.

Table 1: Expected numbers of failures for different situations when the sample size is 80.

True Parameters	Test Plan	Figure 10	Expected Numbers of Failures			
			ξ_L	ξ_M	ξ_H	Total
Original planning values	Optimized	NW	5.7	5.7	20.2	31.6
Original planning values	Recommended	NE	14.1	14.1	12.7	40.9
CPPV	Optimized	SW	2.0	2.0	10.3	14.3
CPPV	Recommended	SE	4.8	4.8	7.4	17.0

6 Concluding Remarks and Areas for Future Research

In this paper, we address the issues involved in planning ALTs with small sample sizes. We describe and investigate the important role that the possibility of zero failures can have on the conditional variance. For constant 3-level ALT plans, using a compromise test plan with an equal expected number of failures at the lowest and middle levels of stress can reduce the ZFP1 probability so that smaller sample sizes become possible for a specified estimation precision and set of planning values. Furthermore, by using the plots of test plans such as those shown in Figure 8, one can select a tentative test plan without having to run time-consuming simulations. Then the tentative test plan needs to be fine-tuned and verified by simulations. Finally, one needs to check whether the commonly-used normal approximation for s-confidence intervals provides an adequate approximation or not.

Due to the small sample sizes involved, there is not a simple theory to provide the actual variance over a large parameter range, as provided by the large sample approximations. However, one may use the strategy outlined in this paper to evaluate and find a good ALT test

plan using simulations. Applying the ideas in this paper to other models and distributions should be straightforward.

In this paper we show how to construct a three-level compromise constant-stress test plan with small sample sizes. If using the smallest number of test units is a primary concern, one might want to use a simple two-level test plan. The planning methods for the three-level constant-stress test plan with small sample sizes can also be used to find a two-level constant-stress test plan with a small sample size. Simulations (for example, [4] and [14]) have shown that the adequacy of large sample approximation is closely related to the expected number of failures. Finally, we point out that it may be more appropriate to replace the term “small samples“ used in this paper as “small expected numbers of failures,” because under certain planning values, the expected number of failures is often small even if large numbers of test units are used.

References

- [1] L. A. Escobar and W. Q. Meeker, “Planning Accelerated Life Tests with Two or More Experimental Factors,” *Technometrics*, vol. 37, pp. 411-422, 1995.
- [2] L. A. Escobar and W. Q. Meeker, “The Large-Sample Approximate Equivalence of the Fisher Information Matrices for Type I and Type II Censored Data from Location-Scale Families,” *Communication of Statistics-Theory: Theory and Methods*, vol. 30, pp. 2211-2225, 2001.
- [3] L. A. Escobar, and W. Q. Meeker, “A Review of Accelerated Test Models,” *Statistical Science*, vol. 21, pp. 552–577, 2006.
- [4] S. L. Jeng, and W. Q. Meeker, “Comparison of Approximate Confidence Interval Procedures for Type I Censored Data,” *Technometrics*, vol. 42, pp. 135-148, 2000.
- [5] W. Q. Meeker, “A Comparison of Accelerated Life Test Plans for Weibull and Lognormal Distributions and Type I Censoring,” *Technometrics*, vol. 26, pp. 157-172, 1984.

- [6] W. Q. Meeker and W. Nelson, "Optimized Accelerated Life Tests for Weibull and Extreme Value Distributions," *IEEE Transactions on Reliability*, vol. 24, pp. 321-322, 1975.
- [7] W. Q. Meeker, and G. J. Hahn, "How To Plan An Accelerated Life Test-Some Practical Guidelines," Volume 10 in *the American Society for Quality Control Basic References in Quality Control: Statistical Techniques*. Milwaukee, Wisconsin: American Society for Quality Control, 1985.
- [8] W. Q. Meeker, and M. J. LuValle, "An Accelerated Life Test Model Based on Reliability Kinetics," *Technometrics*, vol. 37, pp. 133-145, 1995.
- [9] W. Q. Meeker, and L. A. Escobar *Statistical Methods for Reliability Data*, Wiley, New York, 1998.
- [10] W. Q. Meeker, L. A. Escobar, and S. A. Zayac, "Use of Sensitivity Analysis to Assess the Effect of Model Uncertainty in Analyzing Accelerated Life Test Data" in *Case Studies in Reliability and Maintenance*, eds. W. R. Blischke and D. N. P. Murthy, New York: Wiley, Chap 6. 2003.
- [11] W. Nelson, *Accelerated Testing-Statistical Models, Test Plans and Data Analysis*, Wiley, New York, 1990.
- [12] W. Nelson and T. J. Kielpinski, "Theory for Optimized Censored Accelerated Tests for Normal and Lognormal Life Distributions", *Technometrics*, vol. 18, pp. 105-114, 1976.
- [13] W. Nelson and W. Q. Meeker, "Theory for Optimized Censored Accelerated Life Tests for Weibull and Extreme Value Distributions," *Technometrics*, vol. 20, pp. 171-177, 1978.
- [14] S. A. Vander Wiel, and W. Q. Meeker, "Accuracy of Approximate Confidence Bounds Using Censored Weibull Regression Data from Accelerated Life Tests," *IEEE Transactions on Reliability*, vol. 39, pp. 346-351, 1990.